ACS OMEGA

http://pubs.acs.org/journal/acsodf

Article

Characteristics and Stability Assessment of Therapeutic Methionine γ-lyase-Loaded Polyionic Vesicles

Vasily Koval,* Elena Morozova, Svetlana Revtovich, Anna Lyfenko, Arpi Chobanian, Viktoria Timofeeva, Anna Solovieva, Natalya Anufrieva, Vitalia Kulikova, and Tatyana Demidkina

Cite This: *ACS Omega* 2022, 7, 959–967

Read Online

ACCESS | Metrics & More | Article Recommendations

ABSTRACT: Pyridoxal 5′-phosphate-dependent methionine γ-lyase from *Citrobacter freundii* (MGL, EC 4.4.1.11) is studied as an antitumor enzyme and in combination with substrates as an antibacterial agent in enzyme pro-drug therapy. For the possibility of *in vivo* trials, two mutant forms, C115H MGL and V358Y MGL, were encapsulated into polyionic vesicles (PICsomes). Five pairs of polymers with the number of polymer chain units 20, 50, 70, 120, and 160 were synthesized. The effect of polymer length—PEGylated poly-L-aspartic acid and poly-L-lysine—on the degree of MGL incorporation into PICsomes and their size was investigated.

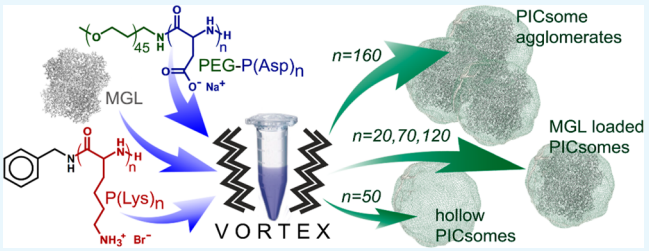

Encapsulation of proteins in PICsomes is a rather new technique. Our data demonstrated that the length of the polymers and, therefore, the ratio of the hydrophobic and hydrophilic fragments most likely should be selected individually for each protein to be encapsulated. The efficiency of encapsulation of MGL mutant forms into PICsomes was up to 11%. The hydrodynamic diameter and surface potential of hollow and MGL-loaded PICsomes were evaluated by the dynamic light scattering method. The size and morphology of the PICsomes were determined by atomic force microscopy. The most acceptable for further *in vivo* studies were $PICsomes_{20}$ with a size of 57−64 nm, $PICsomes_{70}$ of 50−90 nm, and $PICsomes_{120}$ of 100−105 nm. The analysis of the steady-state parameters has demonstrated that both mutant forms retained their catalytic properties inside the nanoparticles. The release study of the enzymes from PICsomes revealed that about 50% of the enzymes remained encapsulated in $PICsomes_{70}$ and $PICsomes_{120}$ after 24 h. Based on the data obtained, the most promising for *in vivo* studies are $PICsomes_{70}$ and $PICsomes_{120}$.

1. INTRODUCTION

Pyridoxal 5′-phosphate-dependent methionine γ-lyase catalyzes the γ-elimination reaction of L-methionine to form α-ketobutyrate, ammonia, and methanethiol.[1] The dependence of tumor cells on exogenous methionine was first shown in 1973.[2,3] Currently, it is believed that the phenomenon called "methionine dependence" may be common to all types of cancer.[4] The antitumor properties of *Pseudomonas putida* MGL have been studied for a long time. There is a comprehensive review on the antitumor effect of *P. putida* enzyme *in vitro*, *in vivo*, and in clinical trials.[5] The mutant form of *Citrobacter freundii* V358Y MGL was shown to inhibit a number of cancer cell lines' growth with a half-maximal inhibitory concentration (IC50) almost twofold lower than the wild-type *C. freundii* MGL does.[6] *C. freundii* MGL also catalyzes the β-elimination reaction of cysteine[7] and its *S*-alk(en)yl substituted sulfoxides to form thiosulfinates, pyruvate, and ammonium.[8,9] Thiosulfinates exhibit antibacterial,[10−14] antitumor,[15−17] and antifungal activities.[13,18]

The application of MGL as an antitumor enzyme and in enzyme pro-drug therapy may be successful if a number of issues are resolved, such as high plasma clearance, short half-life in the bloodstream, and immunogenicity. One of the approaches to get around these limitations is to enclose the enzyme in a lipid or polymeric shell.

The ability of amphiphilic fats and polymers to assemble into hollow vesicles—liposomes and polymersomes—has been shown.[19,20] The advantage of polymersomes lies in a thinner shell, which not only facilitates the transport of a substrate inside but also increases their mechanical and chemical strength.[21] Besides, the ability to modify monomers, influencing the properties of the resulting vesicles such as size, polarity, toxicity, and so forth, is available for polymersomes. There are several ways to obtain such structures, one of which is based on the complexation of polyelectrolytes with different charges.[20] Such a polymersome (PICsome) is a hydrophobic membrane of a polyionic complex located

Received: October 6, 2021
Accepted: December 10, 2021
Published: December 27, 2021

Scheme 1. Synthesis of $pLys_n$ and $PEG\text{-}pAsp_n$

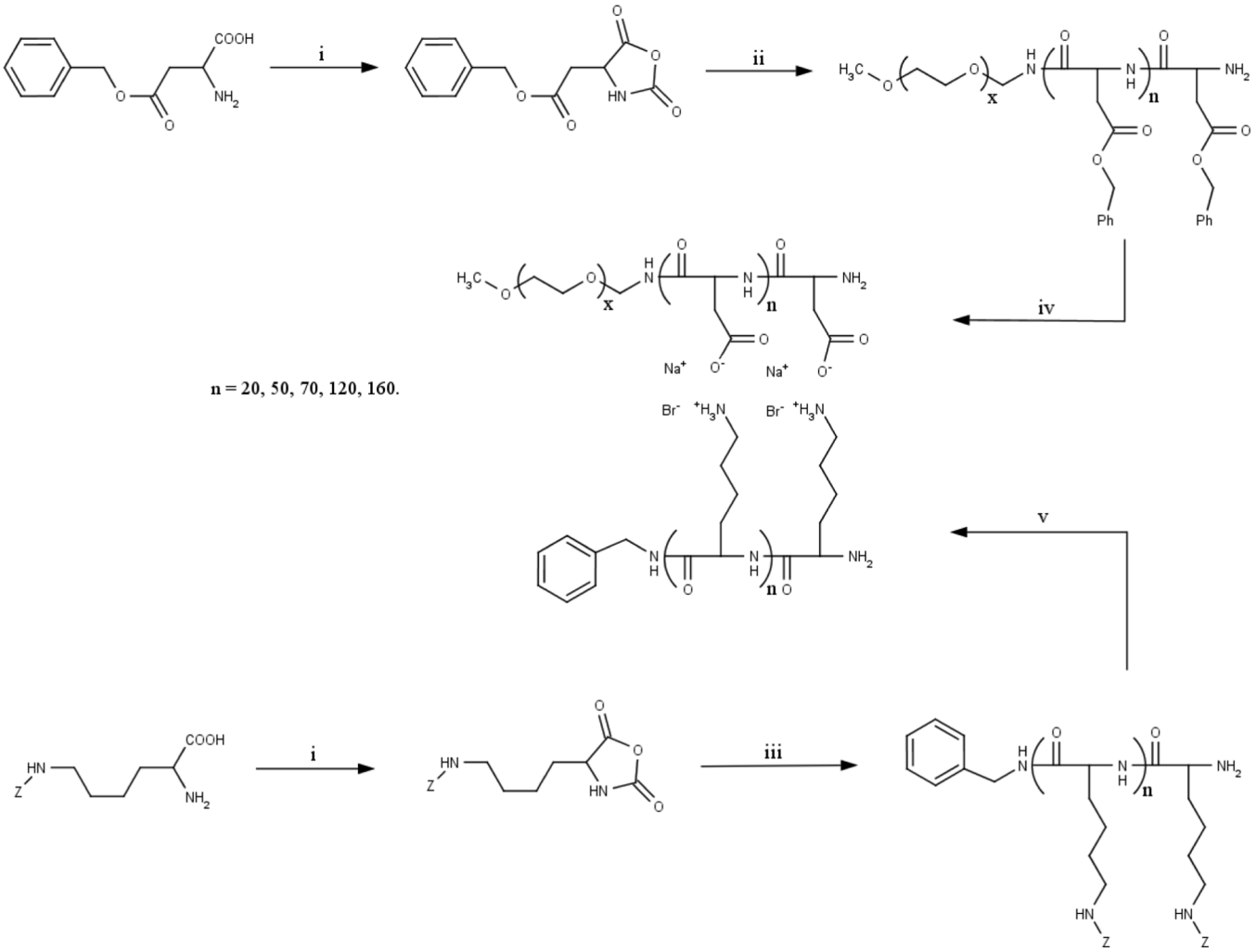

between the hydrophilic blocks of polyethylene glycol.[22,23] This method is particularly suitable for encapsulation of proteins, as it does not require the use of organic solvents or high pH values.

For *in vivo* studies of PICsomes loaded with proteins, it is necessary that their size does not exceed 200 nm. Anraku *et al.* showed that when this value is exceeded, PICsomes suffer from splin capture; moreover, PICsomes with a size of 100−150 nm have the highest mean residence time.[24] The size and shape of PICsomes are influenced by many factors, namely, the ratio of hydrophilic to hydrophobic fragments,[25] the length of the side chain linkers,[26] the concentration of polymers in a solution, and the ionic strength of a medium.[23]

We have shown that the inclusion of C115H MGL into polyionic vesicles significantly improved its pharmacokinetic characteristics.[27] Therapeutic efficacy of the "pharmacological pairs" composed of C115H MGL PICsomes and the substrates *S*-substituted L-cysteine sulfoxides has been demonstrated against the murine model of experimental sepsis caused by the multidrug-resistant *Pseudomonas aeruginosa* 203−2 strain.[28]

Here, we studied the influence of the molecular weight of polyaspartic acid (pAsp) and polylysine (pLys), their concentration, enzyme concentration, and availability of dextran on the PICsome size, their tendency to agglomerate, encapsulation degree of the enzymes, and their release from the vesicles. Steady-state parameters of the β- and γ-elimination reactions catalyzed by encapsulated mutant enzymes were determined.

2. RESULTS AND DISCUSSION

2.1. Polymer Synthesis. To obtain PICsomes, polyaspartic acid (pAsp) was used as anionic and polylysine (pLys) as cationic fragments. The synthesis was carried out by ring-opening polymerization of *N*-carboxyanhydrides of the protected amino acids (Scheme 1) according to the methods described in the literature.[22,30] α-Methoxy-ω-amino polyethylene glycol (MW 1964 g/mol) was used as an initiator for the polymerization of L-aspartic acid *N*-carboxyanhydride (BLA-NCA), and phenylethylamine was used for the polymerization of *Z*-L-lysine *N*-carboxyanhydride.

The degree of polymerization was set by the initiator:monomer ratio determined by ^{1}H NMR spectroscopy. In the case of PEG-pBAsp, the degree of polymerization was determined before deprotection of the carboxylic groups by the ratio of the proton signals of the polyethylene glycol methylene groups at 3.51 ppm and aromatic protons of the benzyl fragment at 7.27 ppm. In the case of pLys, the degree of polymerization was determined after deprotection of amino groups by the signal ratio of the aromatic protons of the initiator at 7.34 ppm and the CH-fragments of polylysine at 4.30 ppm. To increase the

https://doi.org/10.1021/acsomega.1c05558
ACS Omega 2022, 7, 959−967

solubility, polymers were obtained in the form of sodium and hydrobromide salts. Five pairs of polymers were synthesized with the number of polymer chain units 20, 50, 70, 120, and 160.

As mentioned above, MGL is used as an antitumor enzyme[5] and in combination with substrates as an antibacterial pharmacological pair.[10−14] The polylysine chain (Scheme 1) contains the phenyl moiety, which, in addition to being used as an initiator of polymerization and for determining its degree, can be replaced with various fragments for the targeted delivery of the vesicles, such as phytoestrogens,[31,32] steroids,[33] or aptamers.[34]

2.2. Estimation of the Enzyme Inclusion in Nanocapsules. The selection of the optimal conditions for the encapsulation of the enzymes in polyionic vesicles was carried out by varying the concentration of the polymers and the enzyme. The activity of the enzymes in capsules was determined in reactions with L-methionine (V358Y MGL) and *S*-methyl-L-cysteine (C115H MGL). The degree of incorporation of C115H MGL and V358Y MGL labeled with rhodamine was estimated by fluorescence spectroscopy.

First, an optimal concentration of the enzymes for an inclusion was determined. The enzymatic activity of the PICsomes containing the enzymes encapsulated at concentrations from 0.5 to 10 mg/mL was evaluated (Table 1).

Table 1. Selection of Conditions for the Encapsulation of C115H MGL and V358Y MGL

	total activity in $PICsomes_{70}$, U/mL		total activity in $PICsomes_{120}$, U/mL	
MGL concentration	C115H MGL	V358Y MGL	C115H MGL	V358Y MGL
0.5 mg/mL	0.1	0.05	0.08	0.05
1 mg/mL	0.4	0.23	0.56	0.34
2 mg/mL	1.0	0.87	1.2	0.67
4 mg/mL	2.4	1.8	2.1	1.7
6 mg/mL	9.1	7.3	7.8	6.9
8 mg/mL	3.3	1.2	2.3	1.8
10 mg/mL	0.59	1.0	0.9	0.76

It turned out that the best degree of inclusion is achieved at the concentration of 6 mg/mL for both mutant forms.

Second, we investigated the dependence of the length and the concentration of polymeric chains of the PICsomes on the incorporation degree of mutant forms (Table 2).

In each case, the polymers were used in an equimolar ratio of $-COO^-$ and $-NH_3^+$ groups. At polymer concentrations above 1 mg/mL, strong aggregation of the PICsomes was observed. In the case of polymers with 50 units, a very low degree of encapsulation was detected at all concentrations.

2.3. PICsome Size Evaluation. We have previously shown[27] that during the formation of $PICsomes_{70}$, two types of particles were observed—about 50 nm size and >500 nm size. The atomic force microscopy (AFM) image of $PICsomes_{120}$ with encapsulated C115H MGL (Figure 1) contains both individual particles and their agglomerates.

Many methods for preventing the agglomeration of nanocapsules are described, for example, cross-linking of the particles.[35] We tried this method by adding a 1-ethyl-3-(3-dimethylaminopropyl) carbodiimide (EDC) condensing agent to the PICsomes. It was expected that the nanoparticles would become more resistant to changes in the pH and salt content

Table 2. Influence of Concentration and Length of Polymers on the Degree of Encapsulation of C115H MGL and V358Y MGL in PICsomes

		the degree of MGL inclusion in nanocapsules, %[a]	
number of polymer chain links	polymer concentration in reaction mixture	C115H	V358Y
20	1 mg/mL	3.7 ± 0.2	9.1 ± 0.8
	0.5 mg/mL	1.5 ± 0.1	7.3 ± 0.7
	0.1 mg/mL	1.2 ± 0.1	7.2 ± 0.7
50	1 mg/mL	0.1 ± 0.01	0.6 ± 0.05
	0.5 mg/mL	0.05 ± 0.01	0.1 ± 0.01
	0.1 mg/mL	0.04 ± 0.005	0.08 ± 0.01
70	1 mg/mL	10 ± 0.9	3.9 ± 0.3
	0.5 mg/mL	2.5 ± 0.2	1.7 ± 0.1
	0.1 mg/mL	1.7 ± 0.1	1.5 ± 0.1
120	1 mg/mL	11 ± 1	4.1 ± 0.4
	0.5 mg/mL	2.6 ± 0.2	2 ± 0.2
	0.1 mg/mL	1.2 ± 0.1	1.9 ± 0.2
160	1 mg/mL	10 ± 1	2.6 ± 0.2
	0.5 mg/mL	2.4 ± 0.2	0.8 ± 0.07
	0.1 mg/mL	0.3 ± 0.02	0.2 ± 0.02

[a]Average values of experiments which were made in triplicates.

of the solution due to the formation of many carboxamide bonds, but unfortunately, this led to an inactivation of the enzymes. Another method based on coating nanoparticles with an amphiphilic polymer was tested. Rahman *et al.*[36] showed that coating of the nanoparticles with polyethylene glycol prevents agglomeration. However, PEG is a part of PICsomes, and the addition of a new one can lead to a destabilization of their structure. It was decided to use dextran, a polysaccharide used in medicine, as an anticoagulant.[37] In addition, dextran has previously been shown to prevent the agglomeration of superparamagnetic iron oxide nanoparticles.[38] AFM images of $PICsomes_{70}$ with encapsulated C115H MGL without and with the addition of dextran are shown in Figures 2 and 3.

The hydrodynamic diameter and surface potential of the PICsomes were determined after the addition of dextran and centrifugation for 10 min at 5000 rpm (Table 2). Particles not exceeding 200 nm are considered as optimal for *in vivo* studies.[24] PICsomes satisfying these limitations were obtained in the case of polymers with the chain lengths of 20, 70, and 120. Particles with a low *Z*-potential are able to combine, aggregate, and form unstable systems. Correlation of the large size of $PICsomes_{50}$ and $PICsomes_{160}$ and their low *Z*-potential was demonstrated (Table 3). AFM images of these PICsomes also showed the tendency of aggregation even after the addition of dextran (data not shown). In general, the addition of dextran allowed avoiding the formation of agglomerates.

2.4. Steady-State Kinetics of Encapsulated C115H MGL and V358Y MGL and Their Release from the PICsomes. The steady-state catalytic parameters of the γ-elimination reaction of L-methionine, catalyzed by encapsulated V358Y MGL, and the β-elimination reaction of *S*-methyl-L-cysteine, catalyzed by encapsulated C115H MGL, were obtained (Table 4). We tested PICsomes with 20, 70, and 120 polymer chain lengths as more prospective regarding their size and encapsulation degree.

Reaction rates reduced several times as compared to nonencapsulated enzymes: k_{cat} value was observed to be almost 11-fold less for V358Y-PIC_{20}, whereas for V358Y-PIC_{70}

https://doi.org/10.1021/acsomega.1c05558
ACS Omega 2022, 7, 959−967

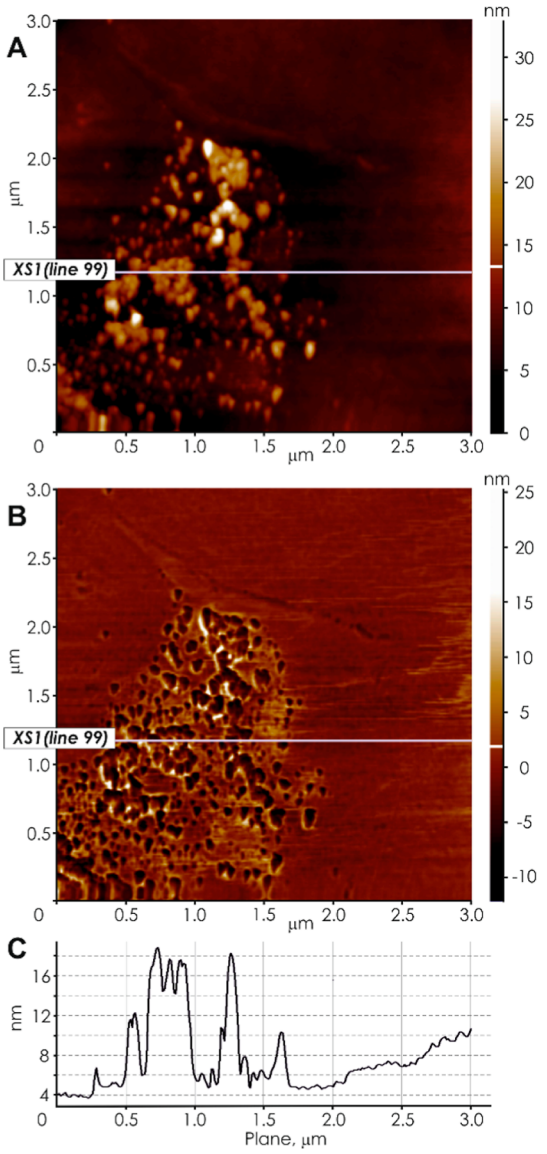

Figure 1. AFM image of a 3 × 3 μm surface fragment, typical appearance of PICsome$_{120}$ with encapsulated C115H MGL, (a) topography, (b) phase images, and (c) cross-section. The concentration of the sample was 1 ng/mL.

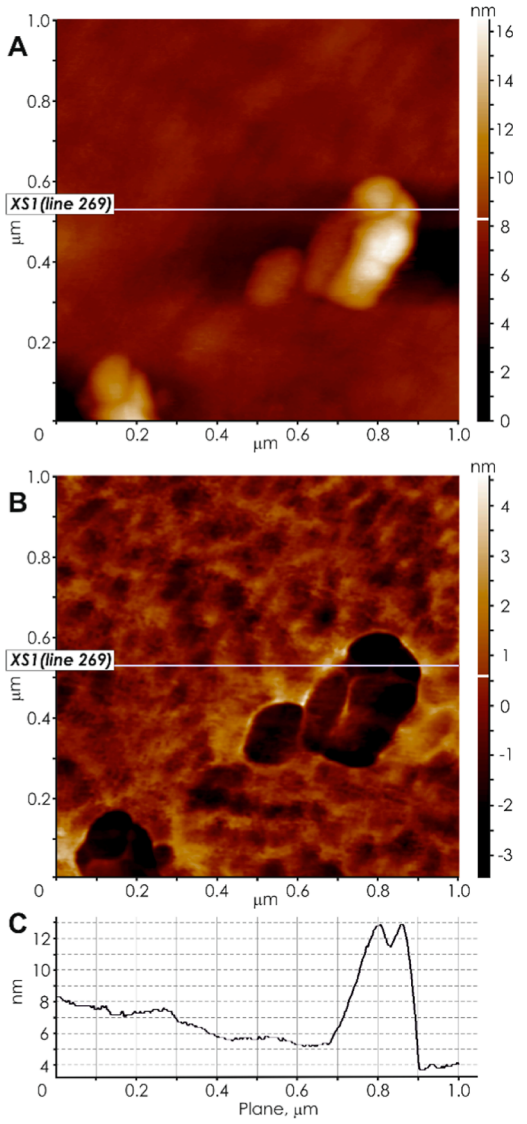

Figure 2. AFM image of a 1 × 1 μm surface fragment, typical appearance of PICsome$_{70}$ with encapsulated C115H MGL, (a) topography, (b) phase images, and (c) cross-section. The concentration of the sample was 1 ng/mL.

and V358Y-PIC$_{120}$, k_{cat} values decreased 2−4 times. The K_m values of L-methionine remained the same or decreased by 2−3 times as compared to the naked enzyme. For encapsulated C115H MGL, catalytic parameters were similar to those determined for the naked MGL (Table 3). The k_{cat} values of *S*-methyl-L-cysteine breakdown did not change much or decrease 3−4 times, and the K_m values proved to be almost the same. In general, both mutant forms retained their catalytic properties inside the nanoparticles, which is promising for using PICsomes in *in vivo* studies.

As shown in Figure 4, after 24 h, the released amount of C115H MGL was found to be 80% from PICsomes$_{20}$, 67% from PICsomes$_{70}$, and 50% from PICsomes$_{120}$.95% of V358Y MGL was released in 24 h from PICsomes$_{20}$, 67% from PICsomes$_{70}$, and 56% from PICsomes$_{120}$. The specific activity of the enzymes inside the PICsomes was tested, and it remained unchanged for 24 h. PICsomes$_{120}$ and PICsomes$_{70}$ retained about 50% of the enzymes during 24 h, allowing the use of such systems for drug delivery.

3. CONCLUSIONS

A set of five pairs of polymers with chain lengths of 20, 50, 70, 120, and 160 units was synthesized with the potential to introduce the desired fragments into their structure, allowing targeted delivery of the vesicles. The optimal concentration of the enzymes and polymers for encapsulation was determined as 6 mg/mL and 1 mg/mL, respectively. PICsome agglomeration was significantly reduced by the addition of dextran. The extent of C115H MGL and V358Y MGL release from PICsomes and the steady-state parameters of the β- and γ-elimination reactions catalyzed by encapsulated mutant forms were determined. PIComes$_{70}$ and PIComes$_{120}$ turned out to be the most promising for further *in vivo* studies due to the relatively high degree of encapsulation—10−11% for C115H MGL and 4% for V358Y MGL, the size not exceeding 105 nm—and the lowest degree of enzyme release.

https://doi.org/10.1021/acsomega.1c05558
ACS Omega 2022, 7, 959−967

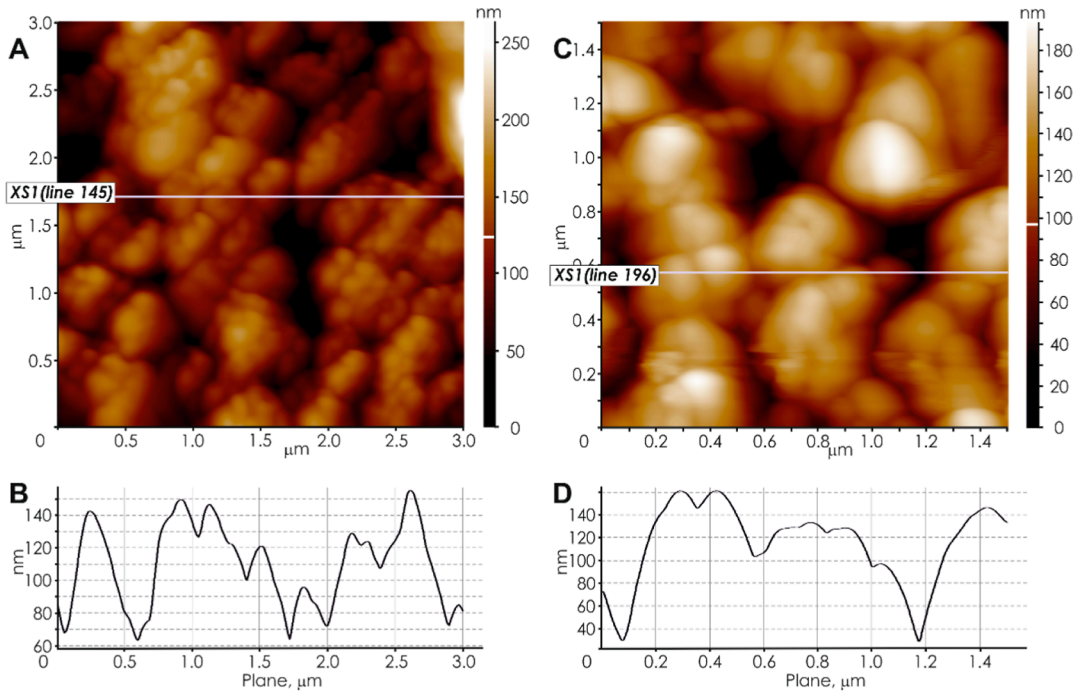

Figure 3. AFM image of a 3 × 3 μm surface fragment, typical appearance of PICsome$_{70}$ with encapsulated C115H MGL and dextran, (a,c) topography, and (b,d) cross-section. The concentration of the sample was 1 ng/mL.

Table 3. Characteristics of the PICsomes after Dextran Addition

	C115H PICsomes		V358Y PICsomes	
number of polymer chain links	diameter, nm	mean Z-potential, mV	diameter, nm	mean Z-potential, mV
20	56.8	−18.93	63.7	−17.9
50	980.1	−5.1	998.2	−3.8
70	50.2	−12.8	90.8	−15.3
120	105.2	−12.3	98.8	−12.39
160	955	−6.85	707.4	−7.5

4. MATERIALS AND METHODS

4.1. Materials. *S*-methyl-L-cysteine, L-methionine, L-aspartic acid, HBr in AcOH, diphosgene, triphosgene, EDC, lactate dehydrogenase, *ε*-*Z*-lysine, tetrahydrofuran (THF), EtOAc, hexane, DMAc, dimethylformamide (DMF), pyridoxal 5′-phosphate, CF_3COOH, dialysis tubing (2000 MWCO), pyridine, and dextran from *Leuconostoc mesenteroides* (MW 35,000−45,000) were purchased from "Sigma−Aldrich" (Germany), NHS-rhodamine was from "Thermo Scientific" (USA), MeO-PEG-NH_2 was purchased from "Iris Biotech GmbH" (Germany), and BzOH, phenylethylamine, NaOH, C_{act}, P_2O_5, Et_2O, H_2SO_4, CH_3CN, CH_2Cl_2, and EtOH were purchased from "Ruskhim" (Russia). The plasmid with the gene of D-2-hydroxyisocaproate dehydrogenase was a kind gift of K. Muratore (University of California, Berkeley, USA). The size of nanocapsules was estimated by dynamic light scattering based on the method of phase analysis of scattered light on a ZETAPLUS BTC (DLS) device. NMR spectra were recorded on "Bruker Avance III HD 300" (Germany).

AFM imaging of the C115H-PICsomes and V358Y-PICsomes on silicon substrates was performed in the semicontact mode with a Solver P47 AFM instrument (NT-MDT, Russia).

Kinetic parameters of the naked and encapsulated enzymes and the amount of rhodamine groups attached to C115H MGL and V358Y MGL were determined using a Cary-50 spectrophotometer (Varian, USA).

The degree of incorporation of the enzymes into PICsomes was determined using a Cary Eclipse spectrofluorimeter (Agilent Technologies, USA) as described in the literature.[24]

4.2. Synthesis of Polymers with Different Numbers of Links in a Chain. *4.2.1. β-Benzyl-L-aspartate.* 10 mL of sulfuric acid and 100 mL (0.89 mol) of benzyl alcohol were successively added to 100 mL of diethyl ether with cooling and stirring. 13.3 g (0.1 mol) of L-aspartic acid was added to the mixture, stirred for 4 h, and left overnight at room temperature. Next, 200 mL of ethyl alcohol was added to the mixture and 50 mL of pyridine dropwise within 2 h. The reaction mixture was left overnight at 4 °C. The resulting white precipitate was filtered off, washed three times with diethyl ether, and

Table 4. Kinetic Parameters of Naked and Encapsulated V358Y MGL and C115H MGL[a]

	V358Y MGL[b]		V358Y-PICsomes$_{20}$		V358Y-PICsomes$_{70}$		V358Y-PICsomes$_{120}$	
substrate	k_{cat}, s^{-1}	K_m, mM	k_{cat}, s^{-1}	K_m, mM	k_{cat}, s^{-1}	K_m, mM	k_{cat}, s^{-1}	K_m, mM
L-methionine	34.2	1.2	3.0	1.0	13.8	0.6	7.6	0.3
	C115H MGL[b]		C115H-PICsomes$_{20}$		C115H-PICsomes$_{70}$		C115H-PICsomes$_{120}$	
S-methyl-L-cysteine	23.1	2.6	30.4	1.6	6.4	2.4	5.6	2.4

[a]The mean squared error of the experiments were within 10%. [b]Data from ref 6. Data from ref 14.

https://doi.org/10.1021/acsomega.1c05558
ACS Omega 2022, 7, 959−967

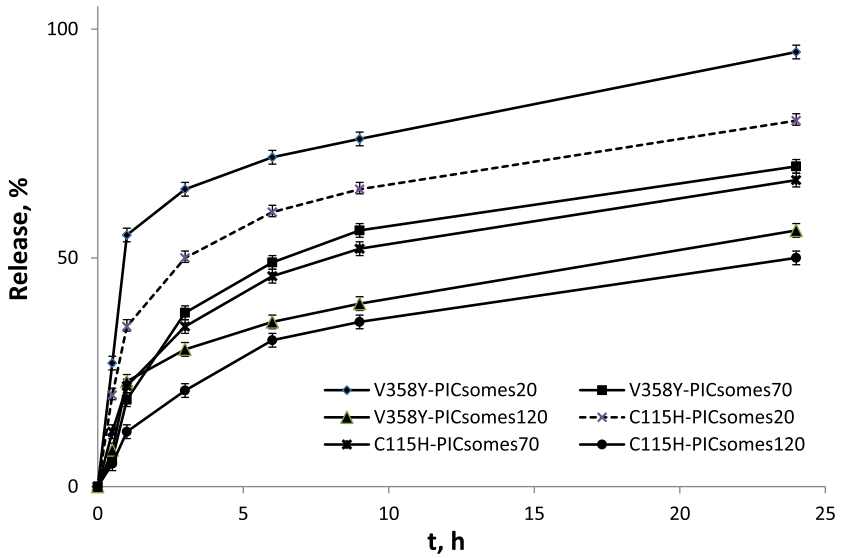

Figure 4. Release of C115H MGL and V358Y MGL from the PICsomes. The values are the average of three independent replicates. Vertical bars indicate the standard errors.

crystallized from water with the addition of 40 μL of pyridine. The yield of the product in the form of a white powder was 9.6 g (43%). m.p. 219−220 (lit. 218−220[29]).

4.2.2. β-Benzyl-L-aspartate-N-carboxyanhydride. 3 g (13.5 mmol) of β-benzyl-L-aspartate and 100 mg of activated carbon were suspended in 30 mL of absolute THF. A solution of 3.24 mL (27 mmol) of diphosgene in 10 mL of THF was added dropwise to the suspension within 30 min. The reaction mass was heated for 30 min at a temperature of 50−55 °C until the starting material was completely dissolved, the coal was separated by filtration, and the solution was evaporated in vacuum. The resulting solid residue was dissolved in ethyl acetate and 50 mL of hexane was added and left overnight at 4 °C. The white crystalline precipitate was filtered off and crystallized twice from the ethyl acetate/hexane mixture. The yield of the product in the form of white crystals was 2.2 g (66%). m.p. 126−127 (decomp).

^{1}H-NMR (DMSO-d_6): 2.86 (dd, J_1 = 17.8 Hz, J_2 = 4.3 Hz 1H, CH_2a), 3.06 (dd, J_1 = 17.8 Hz, J_2 = 4.3 Hz 1H, CH_2b), 4.70 (m, 1H, CH), 5.15 (s, 2H, Ph-CH_2), 7.32 (m, 5H, ArH), 8.96 (br s, 1H, NH).

4.2.3. Polyethylene Glycol-Poly (β-Benzyl-L-aspartate)$_n$. A suspension of MeO-PEG-NH_2 (MW 1962 g/mol) in a mixture of 1 mL of DMF and 4 mL of methylene chloride was added to 1.8 g (7.2 mmol) of β-benzyl-L-aspartate-*N*-carboxyanhydride in a mixture of 5 mL of DMF and 45 mL of methylene chloride. The reaction mixture was stirred for 40 h at 35 °C in an argon atmosphere. Then, diethyl ether (400 mL) was added to the reaction mass. The formed precipitate was filtered off, washed twice with diethyl ether, and dried over P_2O_5. The degree of polymerization (the number of aspartic acid blocks) was determined from the ratio of the signals of the methylene groups of polyethylene glycol (3.52 ppm) and the signals of the aromatic ring (7.27 ppm) in the NMR spectrum. Number chain links of the polymer depended on the amount of the polymerization initiator (MeO-PEG-NH_2).

PEG-polyBASP$_{20}$: yield 33%. ^{1}H NMR (DMSO-d_6): 2.46−2.89 (45H, $CHCH_2CO$), 3.52 (180H, OCH_2CH_2), 4.62 (20H, COCHNH), 5.01 (41H, $COOCH_2Ph$), 7.27 (102H, $COOCH_2Ph$), 7.96 (19H, COCHNH).

PEG-polyBASP$_{50}$: yield 39%. ^{1}H NMR (DMSO-d_6): 2.48−2.91 (103H, $CHCH_2CO$), 3.52 (180H, OCH_2CH_2), 4.62 (49H, COCHNH), 5.01 (105H, $COOCH_2Ph$), 7.27 (258H, $COOCH_2Ph$), 7.99 (49H, COCHNH).

PEG-polyBASP$_{70}$: yield 48%. ^{1}H NMR (DMSO-d_6): 2.55−2.93 (144H, $CHCH_2CO$), 3.52 (180H, OCH_2CH_2), 4.62 (71H, COCHNH), 5.01 (144H, $COOCH_2Ph$), 7.27 (359H, $COOCH_2Ph$), 8.01 (64H, COCHNH).

PEG-polyBASP$_{120}$: yield 51%. ^{1}H NMR (DMSO-d_6): 2.51−2.91 (261H, $CHCH_2CO$), 3.52 (180H, OCH_2CH_2), 4.61 (125H, COCHNH), 5.01 (247H, $COOCH_2Ph$), 7.27 (603H, $COOCH_2Ph$), 8.09 (119H, COCHNH).

PEG-polyBASP$_{160}$: yield 49%. ^{1}H NMR (DMSO-d_6): 2.45−2.93 (332H, $CHCH_2CO$), 3.52 (180H, OCH_2CH_2), 4.61 (163H, COCHNH), 5.01 (323H, $COOCH_2Ph$), 7.27 (805H, $COOCH_2Ph$), 8.1 (155H, COCHNH).

4.2.4. Polyethylene Glycol-Poly (L-Aspartic acid)$_n$. Polyethylene glycol-poly (β-benzyl-L-aspartate)$_n$ was dissolved in a mixture of acetonitrile: 50% NaOH in a ratio of 1:1 and stirred for 10 h at room temperature; then, the pH of the mixture was adjusted to 7.2. Low-molecular weight impurities were removed by dialysis against water. The polymer solution was evaporated and then re-evaporated three times by adding 10 mL of acetone.

PEG-polyASP$_{20}$: yield 68%. ^{1}H NMR (D_2O, 90 °C): 2.76 (42H, $CHCH_2CO$), 3.7 (180H, OCH_2CH_2), 4.45−4.65 (20H, COCHNH).

PEG-polyASP$_{50}$: yield 73%. ^{1}H NMR (D_2O, 90 °C): 2.76 (98H, $CHCH_2CO$), 3.7 (180H, OCH_2CH_2), 4.45−4.65 (51H, COCHNH).

PEG-polyASP$_{70}$: yield 75%. ^{1}H NMR (D_2O, 90 °C): 2.76 (144H, $CHCH_2CO$), 3.7 (180H, OCH_2CH_2), 4.45−4.65 (68H, COCHNH).

PEG-polyASP$_{120}$: yield 69%. ^{1}H NMR (D_2O, 90 °C): 2.76 (246H, $CHCH_2CO$), 3.7 (180H, OCH_2CH_2), 4.45−4.65 (117H, COCHNH).

PEG-polyASP$_{160}$: yield 51%. ^{1}H NMR (D_2O, 90 °C): 2.76 (322H, $CHCH_2CO$), 3.7 (180H, OCH_2CH_2), 4.45−4.65 (158H, COCHNH).

https://doi.org/10.1021/acsomega.1c05558
ACS Omega 2022, 7, 959−967

4.2.5. ε-Carbobenzoxy-L-lysine N-Carboxyanhydride (Z-L-lysine NCA). A solution of 2.6 mL (21.7 mmol) of diphosgene in 10 mL of THF was gradually added to a suspension of 3 g (10.7 mmol) of ε-carbobenzoxy-L-lysine and 100 mg of activated carbon in 30 mL of abs. THF. The reaction mass was heated for 30 min at 50−55 °C and then separated from the coal and evaporated in vacuum. The resulting solid residue was dissolved in ethyl acetate, hexane was added, and the mixture was left overnight at 4 °C. The crystalline white precipitate was filtered off and crystallized twice from ethyl acetate/hexane mixture. The yield of the product was 3.14 g (96%).

^{1}H NMR (DMSO-d_6): 1.22−1.45 (m, 4H, 2 CH_2), 1.60−1.77 (m, 4H, 2 CH_2), 2.98 (m, 2H, CH_2N), 4.42 (t, 1H, J = 6 Hz, CHN), 5.01 (s, 2H, CH_2O), 7.25−7.38 (m, 5H, ArH), 9.02 (br s, 2H, 2 NH).

4.2.6. Poly (Z-L-lysine)$_n$. 3.14 g of Z-L-lysine NCA were dissolved in 30 mL of absolute dimethylacetamide, a solution of 19.6 μL (0.156 mmol) of phenylethylamine in 5 mL of absolute dimethylacetamide was added, and the mixture was stirred for 40 h under argon atmosphere. 250 mL of diethyl ether was added, and the reaction mass was kept at 4 °C for 12 h. The resulting yellow precipitate was collected and dried under vacuum over P_2O_5.

^{1}H NMR (DMSO-d_6, 90 °C): 1.08−2.09 (m, 6H, 3CH_2), 2.84−3.02 (m, 2H, CH_2NH), 3.64−4.38 (m, 1H, COCHNH), 4.98 (s, 2H, CH_2O), 7.04−7.43 (m, 5H, ArH), 7.65−8.36 (m, 1H, NH).

Signal ratios are given, and the degree of polymerization was determined relative to the phenylethylamine signal after deprotection of the polymer amino groups.

4.2.7. Poly (L-lysine)$_n$. 2.71 g of poly(Z-L-lysine)$_n$ was dissolved with cooling in 50 mL of trifluoroacetic acid; 50 mL of 33% HBr in acetic acid was added, and the mixture was stirred for 1 h. The solution was evaporated under vacuum to a volume of 20 mL and then 250 mL of diethyl ether was added, and the mixture was kept at 4 °C for 12 h. The white precipitate was dissolved in water, and low-molecular weight compounds were removed by dialysis against water. Then, the solution was evaporated and re-evaporated three times with 10 mL of acetone. The degree of polymerization was determined from the ratio of the signals of the aromatic protons of the initiator at 7.3 ppm and CH—proton at 4.30 ppm.

$PolyLys_{20}$: yield 75% ^{1}H NMR (D_2O): 1.15−1.98 (m, 128H, 3CH_2), 2.83−3.13 (br s, 38H, CH_2NH), 4.86−5.21 (br s, 20H, COCHNH), 7.16−7.47 (m, 5H, Ph).

$PolyLys_{50}$: yield 82% ^{1}H NMR (D_2O): 1.22−1.99 (m, 321H, 3CH_2), 2.84−3.15 (br s, 100H, CH_2NH), 4.15−4.44 (br s, 51H, COCHNH), 7.16−7.47 (m, 5H, Ph).

$PolyLys_{70}$: yield 80% ^{1}H NMR (D_2O): 1.20−1.96 (m, 442H, 3CH_2), 2.79−3.12 (br s, 133H, CH_2NH), 4.15−4.43 (br s, 72H, COCHNH), 7.16−7.47 (m, 5H, Ph).

$PolyLys_{120}$: yield 84% ^{1}H NMR (D_2O): 1.17−1.97 (m, 783H, 3CH_2), 2.84−3.15 (br s, 224H, CH_2NH), 4.15−4.44 (br s, 119H, COCHNH), 7.16−7.47 (m, 5H, Ph).

$PolyLys_{160}$: yield 85% ^{1}H NMR (D_2O): 1.14−2.01 (m, 990H, 3CH_2), 2.85−3.16 (br s, 316H, CH_2NH), 4.15−4.44 (br s, 158H, COCHNH), 7.16−7.47 (m, 5H, Ph).

4.3. Purification of V358Y MGL and C115H MGL. The V358Y and C115H mutant forms of MGL from *C. freundii* were obtained and purified according to the methods described in,[6,14] respectively. The specific activity of the preparations was determined in the reactions of β-/γ-elimination of S-methyl-L-cysteine/L-methionine (for C115H MGL and V358Y MGL, respectively), measuring the rate of pyruvate/α-ketobutyrate formation in a coupled reaction with lactate dehydrogenase/D-2-hydroxyisocaproate dehydrogenase by reducing the absorption of NADH at 340 nm (ε = 6220 M^{-1} cm^{-1}) at 37 °C. One unit of enzyme activity was defined as the amount of the enzyme that catalyzes the formation of 1.0 μmol min^{-1} of α-ketobutyrate/pyruvate at pH 8.0, 37 °C.

4.4. Preparation and Characterization of C115H and V358Y MGL-Loaded PICsomes. Polyethylene glycol-poly (L-aspartic acid)$_n$ and poly (L-lysine)$_n$ were dissolved in 50 mM potassium phosphate buffer, pH 6.5 at 1 mg/mL, filtered through a 0.22 μm membrane filter, and incubated for 10 min at 37 °C. The solutions of two polymers were mixed in an equal ratio of $-COO^-$ and $-NH_3^+$ units using vortex mixing for 2 min. The enzyme (6 mg/mL in 10 mM potassium phosphate buffer, pH 6.5) was added, and the mixture was stirred at the same speed for 2 min. To remove non-encapsulated enzyme, the mixture was centrifuged at 12,000 rpm for 5 min and the supernatant was exchanged with 10 mM potassium phosphate buffer, pH 7.4. The absence of the enzyme in a supernatant was checked by the disappearance of the characteristic holoenzyme band at 420 nm in the supernatant spectrum.

4.5. Determination of Enzyme Incorporation into PICsomes. To determine the degree of incorporation of the enzymes into PICsomes consisting of polymers of different lengths, C115H MGL and V358Y MGL before encapsulation were modified with rhodamine. Solutions of C115H MGL and V358Y MGL (10 mg/mL in 0.1 M potassium phosphate buffer, pH 8.0) and 6-carboxytetramethyl rhodamine succinimide ester (10 mg/mL in DMSO) were mixed in a molar ratio of 1:10 and incubated for 1 h at room temperature. Then, the preparation was dialyzed against 0.1 M potassium phosphate buffer, pH 8.0, and loaded into PICsomes as described in 4.4. The amount of rhodamine groups incorporated in tetrameric molecules of two mutant forms was determined using the rhodamine molar extinction coefficient 80,000 $M^{-1} \times cm^{-1}$. C115H MGL and V358Y MGL contained four rhodamine groups per molecule. The loading amount of the enzymes into PICsomes was determined using NHS−Rhodamine excitation and emission wavelengths, E_x/E_m = 522/575 by the rhodamine calibration curve we made.

4.6. Atomic Force Microscopy. The PICsomes were dissolved in deionized water (Milli-Q IQ 7000, "Merck", USA) at a concentration of 0.001 μg/mL. Silicon TESP probes ("Bruker", USA) with a nominal resonant frequency of 300 kHz and a nominal tip radius of 10 nm were used. Detailed 3 × 3 μm topography and phase images were obtained at a scan rate of 0.5 Hz and a 512 × 512 pixels resolution.

4.7. Steady-State Kinetics of Encapsulated C115H MGL and V358Y MGL and Their Release from the PICsomes. Steady-state kinetic parameters of the γ-elimination reaction of L-methionine, catalyzed by encapsulated V358Y MGL, and the β-elimination reaction of S-methyl-L-cysteine, catalyzed by encapsulated C115H MGL, were determined as described earlier.[6,14]

The MGL release from the PICsomes was observed at +37 °C in 10 mM potassium phosphate buffer, pH 7.4 during 24 h. After 0.5, 1, 3, 6, 9, and 24 h of incubation, the samples were centrifuged for 5 min at 12,000 rpm, and the absorption spectra of the supernatants were measured at a wavelength range of 250 to 500 nm. The concentrations of the mutant

https://doi.org/10.1021/acsomega.1c05558
ACS Omega 2022, 7, 959−967

forms in supernatants were determined by the absorbance at 278 nm using the extinction coefficient ($A_{278}^{1\%}$) being 0.8.[14]

AUTHOR INFORMATION

Corresponding Author

Vasily Koval − *FSBIS Engelhardt Institute of Molecular Biology of the Russian Academy of Sciences, Moscow 119991, Russia;* orcid.org/0000-0002-1181-104X; Email: tokojami@yandex.ru

Authors

Elena Morozova − *FSBIS Engelhardt Institute of Molecular Biology of the Russian Academy of Sciences, Moscow 119991, Russia;* orcid.org/0000-0003-2922-2793

Svetlana Revtovich − *FSBIS Engelhardt Institute of Molecular Biology of the Russian Academy of Sciences, Moscow 119991, Russia*

Anna Lyfenko − *FSBIS Engelhardt Institute of Molecular Biology of the Russian Academy of Sciences, Moscow 119991, Russia*

Arpi Chobanian − *FSBIS Engelhardt Institute of Molecular Biology of the Russian Academy of Sciences, Moscow 119991, Russia*

Viktoria Timofeeva − *N. N. Semenov Institute of Chemical Physics of the Russian Academy of Sciences, Moscow 119991, Russia*

Anna Solovieva − *N. N. Semenov Institute of Chemical Physics of the Russian Academy of Sciences, Moscow 119991, Russia*

Natalya Anufrieva − *FSBIS Engelhardt Institute of Molecular Biology of the Russian Academy of Sciences, Moscow 119991, Russia*

Vitalia Kulikova − *FSBIS Engelhardt Institute of Molecular Biology of the Russian Academy of Sciences, Moscow 119991, Russia*

Tatyana Demidkina − *FSBIS Engelhardt Institute of Molecular Biology of the Russian Academy of Sciences, Moscow 119991, Russia*

Complete contact information is available at: https://pubs.acs.org/10.1021/acsomega.1c05558

Funding

The work was supported by the Russian Science Foundation (project no. 20-14-00258).

Notes

The authors declare no competing financial interest.

ACKNOWLEDGMENTS

We are grateful to V.T. and A.S. for help in AFM imaging of the samples and T. Lupanova for evaluation of diameter and *Z*-potential of the PICsomes.

REFERENCES

(1) Tanaka, H.; Esaki, N.; Soda, K. Properties of L-methionine γ-lyase from Pseudomonas ovalis. *Biochemistry* **1977**, *16*, 100−106.

(2) Chello, P. L.; Bertino, J. R. Dependence of 5-methyltetrahydrofolate utilization by L5178Y murine leukemia cells in vitro on the presence of hydroxycobalamin and transcobalamin II. *Cancer Res.* **1973**, *33*, 1898−1904.

(3) Kreis, W.; Hession, C. Biological effects of enzymatic deprivation of L-methionine in cell culture and an experimental tumor. *Cancer Res.* **1973**, *33*, 1866−1869.

(4) Hoffman, R. M. The wayward methyl group and the cascade to cancer. *Cell Cycle* **2017**, *16*, 825−829.

(5) Hoffman, R. M. Development of recombinant methioninase to target the general cancer-specific metabolic defect of methionine dependence: a 40-year odyssey. *Expert Opin. Biol. Ther.* **2015**, *15*, 21−31.

(6) Raboni, S.; Revtovich, S.; Demitri, N.; Giabbai, B.; Storici, P.; Cocconcelli, C.; Faggiano, S.; Rosini, E.; Pollegioni, L.; Galati, S.; Buschini, A.; Morozova, E.; Kulikova, V.; Nikulin, A.; Gabellieri, E.; Cioni, P.; Demidkina, T.; Mozzarelli, A. Engineering methionine γ-lyase from Citrobacter freundii for anticancer activity. *Biochim. Biophys. Acta, Proteins Proteomics* **2018**, *1866*, 1260−1270.

(7) Tanaka, H.; Esaki, N.; Soda, K. A versatile bacterial enzyme: l-methionine γ-lyase. *Enzyme Microb. Technol.* **1985**, *7*, 530−537.

(8) Morozova, E. A.; Revtovich, S. V.; Anufrieva, N. V.; Kulikova, V. V.; Nikulin, A. D.; Demidkina, T. V. Allicin is a suicide substrate of *Citrobacter freundii* methionine γ-lyase: structural bases of inactivation of the enzyme. *Acta Crystallogr.* **2014**, *70*, 3034−3042.

(9) Anufrieva, N. V.; Morozova, E. A.; Kulikova, V. V.; Bazhulina, N. P.; Manukhov, I. V.; Degtev, D. I.; Gnuchikh, E. Y.; Rodionov, A. N.; Zavilgelsky, G. B.; Demidkina, T. V. Sulfoxides, Analogues of L-Methionine and L-Cysteine As Pro-Drugs against Gram-Positive and Gram-Negative Bacteria. *Acta Naturae.* **2015**, *7*, 128−135.

(10) Cavallito, C. J.; Bailey, J. H. Allicin, the antibacterial principle of Allium sativum.I.Isolation, physical properties and antibacterial action. *J. Am. Chem. Soc.* **1944**, *66*, 1950−1951.

(11) Small, L. V.; Bailey, J. H.; Cavallito, C. J. Alkyl thiosulfinates. *J. Am. Chem. Soc.* **1947**, *69*, 1710−1713.

(12) Feldberg, R. S.; Chang, S. C.; Kotik, A. N.; Nadler, M.; Neuwirth, Z.; Sundstrom, D. C.; Thompson, N. H. In vitro mechanism of inhibition of bacterial cell growth by allicin. *Antimicrob. Agents Chemother.* **1988**, *32*, 1763−1768.

(13) Leontiev, R.; Hohaus, N.; Jacob, C.; Gruhlke, M. C. H.; Slusarenko, A. J. Comparison of the Antibacterial and Antifungal Activities of Thiosulfinate Analogues of Allicin. *Sci. Rep.* **2018**, *8*, 6763.

(14) Morozova, E.; Kulikova, V.; Rodionov, A.; Revtovich, S.; Anufrieva, N.; Demidkina, T. Engineered *Citrobacter freundii* methionine γ-lyase effectively produces antimicrobial thiosulfinates. *Biochimie* **2016**, *128−129*, 92−98.

(15) Hirsch, K.; Danilenko, M.; Giat, J.; Miron, T.; Rabinkov, A.; Wilchek, M.; Mirelman, D.; Levy, J.; Sharoni, Y. Effect of purified allicin, the major ingredient of freshly crushed garlic, on cancer cell proliferation. *Nutr. Cancer* **2000**, *38*, 245−254.

(16) Merhi, F.; Auger, J.; Rendu, F.; Bauvois, B. Allium compounds, dipropyl and dimethyl thiosulfinates as antiproliferative and differentiating agents of human acutemyeloid leukemia cell lines. *Biologics* **2008**, *2*, 885−895.

(17) Roseblade, A.; Ung, A.; Bebawy, M. Synthesis and in vitro biological evaluation of thiosulfinate derivatives for the treatment of human multidrug-resistant breast cancer. *Acta Pharmacol. Sin.* **2017**, *38*, 1353−1368.

(18) Appel, E.; Vallon-Eberhard, A.; Rabinkov, A.; Brenner, O.; Shin, I.; Sasson, K.; Shadkchan, Y.; Osherov, N.; Jung, S.; Mirelman, D. Therapy of murine pulmonary aspergillosis with antibody-alliinase conjugates and alliin. *Antimicrob. Agents Chemother.* **2010**, *54*, 898−906.

(19) Torchilin, V. P. Recent advances with liposomes as pharmaceutical carriers. *Nat. Rev.* **2005**, *4*, 145−160.

(20) Zhu, Y.; Yang, B.; Chen, S.; Du, J. Polymer vesicles: Mechanism, preparation, application, and responsive behavior. *Prog. Polym. Sci.* **2017**, *64*, 1−22.

(21) Discher, D. E.; Eisenberg, A. Polymer Vesicles. *Science* **2002**, *297*, 967−973.

(22) Koide, A.; Kishimura, A.; Osada, K.; Jang, W.-D.; Yamasaki, Y.; Kataoka, K. Semipermeable Polymer Vesicle (PICsome) Self-Assembled in Aqueous Medium from a Pair of Oppositely Charged Block Copolymers: Physiologically Stable Micro-/Nanocontainers of Water-Soluble Macromolecules. *J. Am. Chem. Soc.* **2006**, *128*, 5988−5989.

(23) Anraku, Y.; Kishimura, A.; Oba, M.; Yamasaki, Y.; Kataoka, K. Spontaneous Formation of Nanosized Unilamellar Polyion Complex Vesicles with Tunable Size and Properties. *J. Am. Chem. Soc.* **2010**, *132*, 1631−1636.
(24) Anraku, Y.; Kishimura, A.; Kobayashi, A.; Oba, M.; Kataoka, K. Size-controlled long-circulating PICsome as a ruler to measure critical cut-off disposition size into normal and tumor tissues. *Chem. Commun.* **2011**, *47*, 6054−6056.
(25) Antonietti, M.; Forster, S. Vesicles and Liposomes: A Self-Assembly Principle Beyond Lipids. *Adv. Mater.* **2003**, *15*, 1323−1333.
(26) Chuanoi, S.; Kishimura, A.; Dong, W.-F.; Anraku, Y.; Yamasaki, Y.; Kataoka, K. Structural factors directing nanosized polyion complex vesicles (Nano-PICsomes) to form a pair of block aniomer/homo catiomers: studies on the aniomer segment length and the catiomer side-chain structure. *Polym. J.* **2014**, *46*, 130−135.
(27) Morozova, E. A.; Kulikova, V. V.; Anufrieva, N. V.; Minakov, A. N.; Chernov, A. S.; Telegin, G. B.; Revtovich, S. V.; Koval, V. S.; Demidkina, T. V. Methionine γ-lyase in enzyme prodrug therapy: An improvement of pharmacokinetic parameters of the enzyme. *Int. J. Biol. Macromol.* **2019**, *140*, 1277−1283.
(28) Morozova, E.; Kulikova, V.; Koval, V.; Anufrieva, N.; Chernukha, M.; Avetisyan, L.; Lebedeva, L.; Medvedeva, O.; Burmistrov, E.; Shaginyan, I.; Revtovich, S.; Demidkina, T. Encapsulated Methionine γ-Lyase: Application in Enzyme Prodrug Therapy of *Pseudomonas aeruginosa* Infection. *ACS Omega* **2020**, *5*, 7782−7786.
(29) Benoiton, L. A synthesis of isoasparagine from β-benzyl aspartate. *Can. J. Chem.* **1962**, *40*, 570−572.
(30) Yu, H.; Chen, X.; Lu, T.; Sun, J.; Tian, H.; Hu, J.; Wang, Y.; Zhang, P.; Jing, X. Poly(l-lysine)-Graft-Chitosan Copolymers:Synthesis ,Characterization ,and Gene Transfection Effect. *Biomacromolecules* **2007**, *8*, 1425−1435.
(31) Appel, E.; Rabinkov, A.; Neeman, M.; Kohen, F.; Mirelman, D. Conjugates of daidzein-alliinase as a targeted pro-drug enzyme system against ovarian carcinoma. *J. Drug Targeting* **2011**, *19*, 326−335.
(32) Lehtonen, J. Y.; Adlercreutz, H.; Kinnunen, P. K. Binding of daidzein to liposomes. *Biochim. Biophys. Acta* **1996**, *1285*, 91−100.
(33) Mishra, P.; Gulbake, A.; Jain, A.; Vyas, S.; Jain, S. Targeted delivery of an anti-cancer agent via steroid coupled liposomes. *Drug Delivery* **2009**, *16*, 437−447.
(34) He, F.; Wen, N.; Xiao, D.; Yan, J.; Xiong, H.; Cai, S.; Liu, Z.; Liu, Y. Aptamer-Based Targeted Drug Delivery Systems: Current Potential and Challenges. *Curr. Med. Chem.* **2020**, *27*, 2189−2219.
(35) Georgilis, E.; Abdelghani, M.; Pille, J.; Aydinlioglu, E.; van Hest, J. C. M.; Lecommandoux, S.; Garanger, E. Nanoparticles based on natural, engineered or synthetic proteins and polypeptides for drug delivery applications. *Int. J. Pharm.* **2020**, *586*, 1−63.
(36) Rahman, M.; Laurent, S.; Tawil, N.; Yahia, L.; Mahmoudi, M. *Protein-Nanoparticle Interactions*; Springer Series in Biophysics; Springer: Berlin, Heidelberg, 2013.
(37) Raucourt, E.; Mauray, S.; Chaubet, F.; Maiga-Revel, O.; Jozefowicz, M.; Fischer, A. Anticoagulant activity of dextran derivatives. *J. Biomed. Mater. Res.* **1998**, *41*, 49−57.
(38) Bilyy, R.; Unterweger, H.; Weigel, B.; Dumych, T.; Paryzhak, S.; Vovk, V.; Liao, Z.; Alexiou, C.; Herrmann, M.; Janko, C. Inert Coats of Magnetic Nanoparticles Prevent Formation of Occlusive Intravascular Co-aggregates With Neutrophil Extracellular Traps. *Front. Immunol.* **2018**, *9*, 2266.

https://doi.org/10.1021/acsomega.1c05558
ACS Omega 2022, 7, 959−967